



HHS Public Access

Author manuscript

Ultrasound Med Biol. Author manuscript; available in PMC 2023 May 01.

Published in final edited form as:

Ultrasound Med Biol. 2022 May ; 48(5): 954–960. doi:10.1016/j.ultrasmedbio.2022.01.007.

Polyvinyl Alcohol Cryogels for Acoustic Characterization of Phase Change Contrast Agents

Phillip G. Durham^{*,1,2}, Jinwook Kim², Katherine M. Eltz², Charles F. Caskey³, Paul A. Dayton^{1,2}

¹Department of Pharmacoengineering and Molecular Pharmaceutics, Eshelman School of Pharmacy, University of North Carolina at Chapel Hill, North Carolina 27599, USA

²Joint Department of Biomedical Engineering, University of North Carolina and North Carolina State University, Chapel Hill, North Carolina 27599, USA

³Vanderbilt University Institute of Imaging Science, Vanderbilt University, Nashville, TN, USA; Department of Radiology and Radiological Sciences, Vanderbilt University Medical Center, Nashville, TN, USA.

Abstract

Phase-change contrast agents (PCCAs) consisting of lipid-encapsulated low-boiling point perfluorocarbons can be used in conjunction with ultrasound for diagnostic and therapeutic applications. One benefit of PCCAs is site-specific activation, whereby the liquid core is acoustically vaporized into a bubble detectable via ultrasound imaging. For further evaluation of PCCAs in a variety of applications, it is useful to disperse these nanodroplets into an acoustically compatible stationary matrix. However, many traditional phantom preparations require heating, which causes premature thermal activation of low-boiling point PCCAs. Polyvinyl alcohol (PVA) cryogels do not require heat to set. Here we propose a simple method for the incorporation of the low-boiling point PCCAs utilizing octafluoropropane (OFP) and decafluorbutane (DFB) into PVA cryogels for a variety of acoustic characterization applications. We then demonstrate the utility of the phantoms by activating droplets with a focused transducer, visualizing the lesions with ultrasound imaging. At 1 MHz, consistent droplet activation was consistently observed at 2.0 MPa and 4.0 MPa for OFP and DFB respectively.

Keywords

Phase-change contrast agent; PCCA; nanodroplets; PVA cryogel

*Corresponding Author: Phillip G. Durham, pgdurham@email.unc.edu, 919-777-4440, 9104 Mary Ellen Jones, 116 Manning Drive, Chapel Hill, NC 27599.

Publisher's Disclaimer: This is a PDF file of an unedited manuscript that has been accepted for publication. As a service to our customers we are providing this early version of the manuscript. The manuscript will undergo copyediting, typesetting, and review of the resulting proof before it is published in its final form. Please note that during the production process errors may be discovered which could affect the content, and all legal disclaimers that apply to the journal pertain.

INTRODUCTION

Gas filled microbubbles are often used in combination with ultrasound as an imaging contrast agent. Additionally, exciting microbubbles with ultrasound at specific acoustic parameter ranges can result in numerous biological effects that are useful in therapeutic applications, such as drug delivery to the brain (O'Reilly and Hynynen 2012), and enhanced high-intensity focused ultrasound ablation (Cheng et al. 2017). The addition of the microbubble amplifies the acoustic energy and allows reduced acoustic power, minimizing off-target effects (Cheng et al. 2017; Kajiyama et al. 2009). While there are many useful applications of microbubbles combined with ultrasound, the functional lifetime of microbubbles in circulation is limited to minutes (Fix et al. 2018; Mullin et al. 2011), and their large size results in confinement within the blood vessels (Gessner et al. 2012).

Liquid-core perfluorocarbon (PFC) emulsions represent an alternate formulation of the traditional microbubble. The application of PFCs that can be induced to undergo a phase change under experimental conditions has led to the development of the Phase Change Contrast Agent (PCCA). PCCAs can be converted from a weakly echogenic droplet into an acoustically responsive microbubble with the application of ultrasound, in a process called acoustic droplet vaporization (ADV) (Apfel 1998; Kripfgans et al. 2000; Kripfgans et al. 2004; Rapoport et al. 2009). These particles therefore retain their microbubble functionality, but benefit from substantially increased circulation lifetimes prior to activation (Sheeran et al. 2015). Other notable advantages of certain PCCAs include the potential to leave the vasculature if manufactured with sufficiently small size distribution, such as nano-scale PCCAs, as well as their uniquely identifiable acoustic activation signature (Sheeran et al. 2014). Furthermore, their selective activation potential, resulting in phase conversion to an acoustically active state only after sufficient energy deposition, makes them useful for HIFU and local targeting applications (Moyer et al. 2015). Due to these advantages, phase change contrast agents are a growing research interest for ultrasound therapy and imaging applications, many of which have been reviewed recently (Borden et al. 2020; Durham and Dayton 2021; Lea-Banks et al. 2019).

PCCAs consist of a perfluorocarbon core surrounded by a shell material. The properties of both components play a role in the PCCA activation profile and subsequent stability. Many factors affect the pressure required for ADV, such as droplet size, evaluation temperature, perfluorocarbon core, ultrasound frequency and duty cycle (Aliabouzar et al. 2019; Fabiilli et al. 2009; Kripfgans et al. 2004; Shpak et al. 2014). Conventionally, perfluorocarbon emulsions have been made using perfluorocarbons that are liquid at room temperature formulation conditions. However, these require substantial ultrasound pressure to vaporize (Fabiilli et al. 2009) which is typically above approved imaging guidelines and beyond the capability of many clinical imaging systems. Newer formulation methods have been developed for the generation of PCCAs using low-boiling point PFCs that have lower temperature and activation pressure thresholds, making them more accessible for *in vivo* imaging and therapy applications (Sheeran et al. 2011b; Sheeran et al. 2012).

As applications of low-boiling point PCCAs are investigated, it is useful to have a consistent method of evaluating different PCCAs in ultrasound applications. Traditionally, PCCAs have

Author Manuscript
Author Manuscript
Author Manuscript
Author Manuscript

been evaluated in acoustically transparent tubes (Arena et al. 2015), OptiCells (Shpak et al. 2014), or other systems whereby the agents are able to freely circulate. However, these models do not simulate the boundary conditions or attenuation from surrounding tissue, nor do they necessarily constrain agent motion. In situations where it is desired to constrain the droplets and/or surround them with attenuating material, PCCAs can be incorporated into a gel-based ultrasound phantom. Traditional higher boiling point PCCAs have been evaluated in this manner. Dodecafluoropentane (DDFP), which has a boiling point of 28°C, droplets incorporated into a polyacrylamide phantom has allowed extensive characterization of droplet activation following exposure to various ultrasound parameters (Williams et al. 2013). Similarly, DDFP embedded in acrylamide was used to generate spherical point targets for ultrasound imaging following ADV (Carneal et al. 2011). While these PCCA-embedded phantoms are fairly straightforward using PFCs with high boiling points, they become problematic for low-boiling point PCCAs. Many ultrasound phantom procedures require heat either in the dissolution and setting of the hydrogel material (in the case of gelatin and agar) or an exothermic chemical crosslinking process (e.g. polyacrylamide). Due to the temperature sensitivity of low boiling point PCCAs, these methods may result in premature activation or a decrease in suspended PCCA concentration. Therefore a method to generate a thermostable ultrasound phantom that does not expose PCCAs to elevated temperatures is desirable.

Polyvinyl alcohol (PVA) is a non-toxic, water soluble and biodegradable synthetic polymer which has many industrial uses. Aqueous solutions of PVA can be gelled by freezing and thawing the solution to form a polyvinyl alcohol cryogel (PVA-C). PVA-C material properties are affected by thermal history. Repeated freezing and thawing allow for the formation of physical crosslinks due to polymer phase separation from water in the thawing process (Wan et al. 2014). This results in a mesh-like polymer network consisting of semicrystalline polymeric regions and pores. Previous studies have demonstrated a clear relationship of increasing mechanical properties with increasing numbers of freeze and thaw cycles (Surry et al. 2004; Wan et al. 2014). Similarly, investigations of PVA-C for ultrasound applications have also found that increasing the number of freeze-thaw cycles correlates to increasing speed of sound and attenuation of unmodified PVA-C (Fromageau et al. 2003; Surry et al. 2004). Like many hydrogels used for the construction of ultrasound phantoms, PVA-C alone does not have substantial scattering or attenuation properties to be tissue-mimicking. However, a variety of additions to PVA-C have been evaluated to grant them tissue-mimicking acoustic properties, such as enamel paint (Surry et al. 2004), silica powder (Fromageau et al. 2003), cellulose (Fromageau et al. 2007), aluminum, graphite and silicon carbide powders (Weir et al. 2015).

We present here a new method of creating ultrasound phantoms which contain PCCAs, gelled without elevated temperatures. The nanodroplet emulsions within thus remain stable during preparation, and can be spatially activated within a wide range of acoustic pressures for the comparison of temperature-sensitive low-boiling point PCCAs in ultrasound applications, including clinical imaging and high-intensity focused ultrasound (HIFU).

MATERIALS AND METHODS

PCCA preparation

Low-boiling point PCCA nanodroplets were prepared as reported previously (Sheeran et al. 2011a). Briefly, a solution of 1,2-distearoyl-sn-glycero-3-phosphocholine (DSPC) and 1,2-distearoyl-sn-glycero-3-phosphoethanolamine-N-[methoxy(polyethylene glycol)-2000] (DSPE-PEG2000) (Avanti Polar Lipids, Birmingham, AL, USA) was prepared in PBS with glycerol and propylene glycol at 9:1 DSPC:DSPE-PEG2000 in a 3mL glass vial. The vial was sealed with a crimp-top butyl septa, then degassed under vacuum for 30 minutes. The vial headspace was backfilled with octafluoropropane (OFP) or decafluorobutane (DFB) gas (FluoroMed L.P., Round Rock, TX, USA). Microbubbles were generated by mechanical agitation of the vial for 45 seconds (Vialmix, Lantheus Medical Imaging, Billerica, MA, USA). Finally, the vial was cooled to -13°C in a chilled ethanol bath and pressurized at 45 pounds per square inch (PSI) via compressed nitrogen in the case of OFP droplets, and 20 PSI for DFB droplets. Droplet size and concentration was determined by single particle optical sizing (AccuSizer FX-Nano, Entegris, Billerica, MA, USA) to be 0.32 μm , 9.89^9 #/mL, and 0.34 μm , 1.25×10^{10} #/mL respectively for OFP and DFB droplets.

Phantom preparation

To prepare the droplet phantoms, 20 grams of PVA (Sigma Aldrich, MW 85,000-124,000) was dissolved in 200 mL (10% PVA w/v) of distilled water with heat (approximately 95°C) and stirring. Once fully dissolved, the viscous PVA solution was covered and cooled to below 30°C while stirring. 200 μL droplets (1 μL droplets per mL PVA solution) were added to the cooled PVA solution and stirred manually, to prevent the formation of bubbles in the solution. The PVA-droplet solution was then exposed to 3 freeze-thaw cycles, each consisting of 12 hours at -20°C followed by 12 hours at 20°C (Supplemental Figure 1).

Droplet-free phantoms ($n=3$) were prepared to characterize the PVA phantoms acoustic properties. A rectangular phantom was prepared following the same procedure with the omission of droplets. Wave speed and attenuation of a PVA phantom was measured by the through-transmission method used in previous work (Surry et al. 2004). Two 1 MHz piston transducers with a diameter of 25.4 mm (IL0108HP, CTS, Hopkinton, MA, USA) were used as a transmitter and a receiver. The two transducers were aligned in a water tank filled with degassed, distilled water ($24.6 \pm 0.2^{\circ}\text{C}$). The distance between the transducers was controlled by a motorized scanning system (Newport XPS, Irvine, CA, USA), and set as 123 mm which is further than the far-field limit of the used piston transducer ($D/4\lambda = 108$ mm, where D and λ denote the diameter and wavelength, respectively) (AIUM Technical Standards Committee 1995). This far-field requirement is to avoid unwanted pressure amplitude variation in a near-field (Surry et al. 2004). The transmitter was driven by an arbitrary function generator (AFG3101, Tektronix Inc., Beaverton, OR, USA) with a 55 dB RF amplifier (A150, E&I, Rochester, NY, USA). The excitation was 100 sinusoidal cycles at 1 MHz, with 20-Hz pulse repetition frequency (PRF). First, burst waves that propagated through water were detected by the receiver, and we acquired the signals as a reference. Second, the PVA phantom was aligned close to the receiver (100 mm away from the transmitter), and burst waves propagated through both water and a phantom were detected

by the receiver. We acquired the detected time-domain signals ($n=10$) and compared them with the reference signal. Each data acquisition was repeated three times ($n=3$).

We compared the difference in time-of-arrival (Δt) of two cases to determine the sound speed of a phantom, c_p , using equation (1), where c_w and d denote the sound speed of water and the phantom thickness (20 mm). The sound speed of the water at 24.6°C was determined by using equation (2), where T is the temperature in °C (AIUM Technical Standards Committee 1995). Next, we compared the maximum amplitude (peak-to-peak) of the two signals to determine the attenuation coefficient, α_p using equation (3), where A_w and A_p denote the peak-to-peak amplitude of water case and phantom case, respectively.

$$c_p = \frac{c_w}{1 + \Delta t \frac{c_w}{d}} \quad (1)$$

$$c_w = 1403 + 5T - 0.06T^2 + 3.0 \times 10^{-4}T^3 \quad (2)$$

$$\alpha_p = \frac{20}{d} \log\left(\frac{A_w}{A_p}\right) \quad (3)$$

PCCA activation via clinical imaging

Imaging and activation were evaluated with a clinical ultrasound scanner (Acuson Sequoia, Siemens Medical Solutions, Malvern, PA, USA) in tissue harmonic B-mode imaging (15L8 probe, transmit at 7 MHz, receive at 14 MHz). A phantom prepared in a cylindrical mold was acclimated to a 20°C water bath on top of an acoustic absorber to limit reflections. The transducer power was lowered to a mechanical index (MI) of 0.20 to initially position the transducer without activating the droplets. Focus was set to 2 cm, approximately 9 mm below the top of the phantom. Videos were acquired at a frame rate of 1 Hz as the output power and mechanical index was slowly incremented to full output power (MI = 1.8). Following activation, output power was reduced to below activation threshold for comparison.

HIFU characterization

To demonstrate the utility of using droplet-loaded PVA phantoms for HIFU characterization, 10% PVA phantoms were prepared with OFP or DFB droplets (boiling points - 37°C and -2°C respectively) at 1 µL/mL, using a 3D printed rectangular mold. After three freeze-thaw cycles, the phantom was treated at 20°C or placed into a heated water bath at 37°C and allowed to equilibrate. Temperature was monitored by inserting a thermocouple into the phantom. High-intensity focused ultrasound was applied via a Philips Therapy and Imaging System (TIPS), an 8-element annular array with an adjustable focal depth and radius of curvature of 80 mm. The imaging transducer was fixed in position in the annulus and focused to the phantom (Supplemental Figure 2). Imaging area was cropped to the phantom. Images were taken at 20 Hz during HIFU exposure of 0.5 – 4.5 MPa peak negative pressure,

100% duty cycle at 1 MHz for a treatment duration of 1 second. After each activation, the phantom was repositioned to an unactivated region. To visualize the resulting droplet activation, the first frame (representing pre-activated phantom) was subtracted from each subsequent frame in the cineloop. Average enhancement was calculated by defining a region of interest around the focal spot and averaging the difference of a pre-activation and a post-activation frame.

RESULTS

Acoustic Characterization of droplet-free PVA phantoms

At 24.6°C, the sound speed in water is 1494.2 m/s. The wave speed of the three independent PVA phantoms was determined to be 1521 m/s, with a standard deviation of ± 2.8 m/s and the attenuation was 1.91 dB/m, with a standard deviation of ± 1.6 dB/m (@1 MHz), across the three measurements. This is a lower attenuation than observed in Surry et al, which found a frequency independent attenuation coefficient of $0.21 \text{ dB} (\text{cm MHz})^{-1}$ for PVA cryogels experiencing 3 freeze thaw cycles (Surry et al. 2004). It should be noted that the attenuation coefficient is frequency-dependent, and it increases as frequency increases. The lowest frequency investigated by Surry et al. was 3 MHz. Since our PVA phantom was designed for therapeutic ultrasound applications that primarily use 1 MHz ultrasound, we determined the attenuation coefficient at 1 MHz. Differences in polymer molecular weight and hydrolysis may also contribute to the differences in attenuation.

OFP droplet activation with a clinical scanner at room temperature

The phantom was a white, opaque firm solid. Morphologically, the phantom had a rounded dome in the center, a result of expansion during freeze in the cylindrical mold. At MI = 0.73, the phantom appeared dark on ultrasound imaging, with little internal structure visible and no pre-activation visible. As MI increased to 1.3, discrete bright areas were visible around the transducer focus where perfluorocarbon droplets had vaporized into microbubbles. This activation area increased with increasing MI (Figure 1). Upon reducing the mechanical index, the activated areas remained visible on b-mode imaging. The activation area expands outward from the focal area with increasing MI, representing an increase in the area of pressure above the activation threshold. The imaging transducer was unable to activate DFB droplets prepared in PVA phantoms at a maximum MI of 1.9.

OFP and DFB droplet activation with focused ultrasound at physiological temperature

For HIFU characterization, imaging was achieved by inserting the transducer into the center of the HIFU transducer annulus. Due to the focal depth of the HIFU transducer, the imaging transducer was operated at maximum depth. Imaging at full depth with low MI, and interference from the focused transducer housing contributed to higher background signal from phantom internal heterogeneity, which was able to be removed via background subtraction in post-processing (Supplemental Figure 3). Above the activation pressure threshold, a distinct lesion was formed upon 1 second exposure to focused ultrasound (Figure 2, Supplemental video 1). Subtracting the first pre-activation frame in each sequence enabled isolation of the activated area for clearer visualization and localization. Droplet activation increased with ultrasound pressure for both OFP and DFB. OFP consistently

showed activation at and above 2 MPa PNP at 20°C, whereas DFB did not show consistent activation until above 4 MPa at 37°C. Above 2.0 MPa, OFP activation displayed a darker central region, potentially caused by destruction of the resulting bubbles due to the high duty cycle and long treatment duration. At 4.5 MPa, OFP droplets increased enhancement beyond the original focal region, resulting in a higher average enhancement.

DISCUSSION

PVA cryogels were fabricated with the inclusion of PCCAs formulated from low boiling point perfluorocarbons OFP (-37°C) and DFB (-2°C) with minimal thermal activation. The droplet-free phantoms prepared under the same methods exhibited low acoustic attenuation. Without attenuation and at room temperature, phantoms containing low-boiling point perfluorocarbons such as OFP could be activated on the principle of pressure alone, without the mitigating effects of local heating due to attenuation.

The phantom presented here consists of polyvinyl alcohol without any additional formulation additives. The mechanical properties of PVA cryogels may impact any one particular application, and others have extensively characterized process parameters that may impact the rigidity of PVA cryogels, such as the length and number of freeze-thaw cycles (Pazos et al. 2009) and the thawing temperature. Three freeze-thaw cycles was chosen for this experiment, as previous experiments demonstrate that the cryogel mechanical properties become more consistent after three cycles (Pazos et al. 2009). While this experiment thawed the samples at 20°, it is possible to further reduce exposure to elevated temperatures by thawing at a lower temperature (i.e. 4°C), though this will have an effect on the mechanical properties of the phantom, with slower thawing resulting in stronger gels (Damshkalan et al. 1999). This approach may be beneficial when using less stable droplets, or to increase mechanical properties using fewer freeze-thaw cycles. This experiment did not specifically determine the effect of repeated freeze-thaw cycles on the nanodroplets other than to visualize activation, which was comparable at the activation threshold for both perfluorocarbons. Freezing and thawing reportedly does not result in significant loss of concentration (Kasoji et al. 2015), but the effects of repeat freezing and thawing in PVA-C could be further investigated.

The total enhancement for OFP and DFB at their respective activation threshold was consistent, representative of droplet activation in the focal zone of the transducer. The activation pressure thresholds of 2.0 MPa for OFP and 4.0 MPa for DFB display a similar trend to previously published observations using the same perfluorocarbon core (1.74 MPa and 3.49 MPa respectively (Li et al. 2019)), though slight differences in droplet shell composition, size distribution and ultrasound parameters prevent a direct comparison. It has been reported that confinement also affects droplet activation (Raut et al. 2019; Rojas et al. 2019). Previous work embedding DDFP also demonstrated the stiffness of the phantom impacts the pressures and/or temperatures required for droplet activation compared to the same droplets in an unencumbered system such as a water bath (Williams et al. 2013). To alter the stiffness of PVA cryogels, the thawing temperature and duration may additionally be controlled. It has been determined that slower thaw rates result in firmer cryogels (Damshkalan et al. 1999; Lozinsky 2002).

Author Manuscript
Author Manuscript
Author Manuscript
Author Manuscript

Regarding modifications to PVA cryogels, it may possible to construct optically clear PVA droplet phantoms following the glycerol addition method of Du Toit et. al. (Du Toit and Pott 2020). Others have investigated acoustic modifications to PVA cryogels in the form of additives which serve to set the speed of sound in the phantom and provide tissue-mimicking attenuation (Surry et al. 2004). As many of these approaches call for the simple inclusion of a scatterer, inclusion of low-boiling point PCCAs into tissue mimicking PVA-C phantoms should also be possible following this method.

Once the droplets are activated, they remained visible on contrast imaging and B-mode below the MI required for activation, allowing for diagnostic evaluation of the beam profile without further activation. Though this has not been extensively characterized, the lesions produced from the DFB phantom with focused activation were still apparent 24 hours after the initial activation following refrigerated storage. Lesions resulting from OFP droplets were not still evident at that time, but no attempt was made in this experiment to optimize lesion longevity and it is possible that this could be improved.

A substantial benefit of PVA cryogels in this application is the ability to apply heat without degrading the gel structure. It is also possible to embed droplets in gelatin, similar to the procedure used in Kim et. al. to embed microbubbles (Kim et al. 2021). The resulting gelatin phantom may have utility for room temperature applications but ultimately will dissolve when heated to physiological temperature in a water bath. No change in PVA-C integrity was observed when heated to 37°C for the duration of the focused ultrasound experiments. Oppositely, polyacrylamide phantoms which have been developed for HIFU studies (Takegami et al. 2004) are able to withstand heating, but the chemical crosslinking process is exothermic which may cause thermal activation of low-boiling point perfluorocarbons during phantom manufacture. Heating to 37°C was required to visualize activation with DFB within the pressure capability of the therapy transducer. However, attempts to heat OFP phantoms to 37°C resulted in dramatically reduced or no activation in the current experiment. This is possibly due to increased time spent at elevated temperature resulting in thermal activation and dissolution. It may be possible to optimize experiments for evaluation of OFP at elevated temperatures, but will require further investigation.

CONCLUSION

Here we describe a system that allows for the embedding of stationary nanodroplets which can be set via freeze/thaw cycles, without elevated thermal exposure to low-boiling point perfluorocarbon phase change contrast agents. Spatial acoustic activation was demonstrated with OFP and DFB nanodroplets at ambient and physiological temperatures. Resulting droplet activation can be visualized during and following vaporization via ultrasound imaging, allowing for acoustic characterization of imaging or focused therapy systems.

Supplementary Material

Refer to Web version on PubMed Central for supplementary material.

Acknowledgement and Competing Interests

The authors wish to thank Brian Velasco for assistance in droplet preparation and Aparna Singh for productive discussions and collaboration. This study was partially supported by NIH R21EB021012 and the Carolina Center for Cancer Nanotechnology Excellence. P.A.D. declares that he is a co-inventor on low-boiling point nanodroplet technology, and a co-founder of Triangle Biotechnology, a company which has licensed this technology from UNC Chapel Hill.

REFERENCES

- AIUM Technical Standards Committee. Methods for Specifying Acoustic Properties of Tissue Mimicking Phantoms and Objects. Laurel, MD: American Institute of Ultrasound in Medicine, 1995.
- Aliabouzar M, Kumar KN, Sarkar K. Effects of droplet size and perfluorocarbon boiling point on the frequency dependence of acoustic vaporization threshold. *J Acoust Soc Am Acoustical Society of America (ASA)*, 2019;145:1105–1116. [PubMed: 30823782]
- Apfel RE. Activatable infusible dispersions containing drops of a superheated liquid for methods of therapy and diagnosis. U.S. Patent and Trademark Office, 1998.
- Arena CB, Novell A, Sheeran PS, Puett C, Moyer LC, Dayton PA. Dual-frequency acoustic droplet vaporization detection for medical imaging. *IEEE Trans Ultrason Ferroelectr Freq Control Institute of Electrical and Electronics Engineers Inc.*, 2015;62:1623–1633.
- Borden MA, Shakya G, Upadhyay A, Song KH. Acoustic Nanodrops for Biomedical Applications. *Curr Opin Colloid Interface Sci Curr Opin Colloid Interface Sci*, 2020;50.
- Carneal CM, Kripfgans OD, Carson PL, Fowlkes JB, Carneal CM, Kripfgans OD, Carson PL, Fowlkes JB, Krücker J. A Tissue-Mimicking Ultrasound Test Object Using Droplet Vaporization to Create Point Targets. *IEEE Trans Ultrason Ferroelectr Freq Control IEEE Trans Ultrason Ferroelectr Freq Control*, 2011;58:2013–2025. [PubMed: 21937339]
- Cheng C, Xiao Z, Huang G, Zhang L, Bai J. Enhancing ablation effects of a microbubble contrast agent on high-intensity focused ultrasound: an experimental and clinical study. *BJOG An Int J Obstet Gynaecol Blackwell Publishing Ltd*, 2017;124:78–86.
- Damshkalin LG, Simenel IA, Lozinsky VI. Study of Cryostructuration of Polymer Systems. XV. Freeze-Thaw-Induced Formation of Cryoprecipitate Matter from Low-Concentrated Aqueous Solutions of Poly(vinyl alcohol). 1999;
- Du Toit JP, Pott RWM. Transparent polyvinyl-alcohol cryogel as immobilisation matrix for continuous biohydrogen production by phototrophic bacteria. *Biotechnol Biofuels BioMed Central Ltd*, 2020;13:1–16. [PubMed: 31911817]
- Durham PG, Dayton PA. Applications of sub-micron low-boiling point phase change contrast agents for ultrasound imaging and therapy. *Curr Opin Colloid Interface Sci Elsevier*, 2021;56:101498.
- Fabiilli ML, Haworth KJ, Fakhri NH, Kripfgans OD, Carson PL, Fowlkes JB. The role of inertial cavitation in acoustic droplet vaporization. *IEEE Trans Ultrason Ferroelectr Freq Control Institute of Electrical and Electronics Engineers Inc.*, 2009;56:1006–1017.
- Fix SM, Nyankima AG, McSweeney MD, Tsuruta JK, Lai SK, Dayton PA. Accelerated Clearance of Ultrasound Contrast Agents Containing Polyethylene Glycol is Associated with the Generation of Anti-Polyethylene Glycol Antibodies. *Ultrasound Med Biol Elsevier*, 2018;44:1266–1280. [PubMed: 29602540]
- Fromageau J, Brusseau E, Vray D, Gimenez G, Delachartre P. Characterization of PVA cryogel for intravascular ultrasound elasticity imaging. *IEEE Trans Ultrason Ferroelectr Freq Control* 2003;50:1318–1324. [PubMed: 14609071]
- Fromageau J, Gennisson JL, Schmitt C, Maurice RL, Mongrain R, Cloutier G. Estimation of polyvinyl alcohol cryogel mechanical properties with four ultrasound elastography methods and comparison with gold standard testings. *IEEE Trans Ultrason Ferroelectr Freq Control* 2007;54:498–508. [PubMed: 17375819]
- Gessner RC, Aylward SR, Dayton PA. Mapping Microvasculature with Acoustic Angiography Yields Quantifiable Differences between Healthy and Tumor-bearing Tissue Volumes in a Rodent Model. *Radiology* 2012;264:733–740. [PubMed: 22771882]

- Kajiyama K, Yoshinaka K, Takagi S, Matsumoto Y. Micro-bubble Enhanced HIFU. *Phys Procedia* 2009;3:305–314.
- Kasoji SK, Pattenden SG, Male EP, Jayakody CN, Tsuruta JK, Mieczkowski PA, Janzen WP, Dayton PA. Cavitation enhancing nanodroplets mediate efficient DNA fragmentation in a bench top ultrasonic water bath. *Public Library of Science*, 2015;10:e0133014.
- Kim J, Kasoji S, Durham PG, Dayton PA. Acoustic holograms for directing arbitrary cavitation patterns. *Appl Phys Lett American Institute of Physics Inc.*, 2021;118:051902.
- Kripfgans OD, Fabiilli ML, Carson PL, Fowlkes JB. On the acoustic vaporization of micrometer-sized droplets. *J Acoust Soc Am Acoustical Society of America (ASA)*, 2004;116:272–281. [PubMed: 15295987]
- Kripfgans OD, Fowlkes JB, Miller DL, Eldevik OP, Carson PL. Acoustic droplet vaporization for therapeutic and diagnostic applications. *Ultrasound Med Biol Elsevier Science Ltd*, 2000;26:1177–1189. [PubMed: 11053753]
- Lea-Banks H, O'Reilly MA, Hyynen K. Ultrasound-responsive droplets for therapy: A review. *J. Control. Release Elsevier B.V.*, 2019. pp. 144–154.
- Li DS, Schneewind S, Bruce M, Khaing Z, O'donnell M, Pozzo L. Spontaneous Nucleation of Stable Perfluorocarbon Emulsions for Ultrasound Contrast Agents. *Nano Lett* 2019;19:173–181. [PubMed: 30543289]
- Lozinsky VI. Cryogels on the basis of natural and synthetic polymers: Preparation, properties and application. *Usp Khim IOP Publishing*, 2002;71:579–584.
- Moyer LC, Timbie KF, Sheeran PS, Price RJ, Miller GW, Dayton PA. High-intensity focused ultrasound ablation enhancement in vivo via phase-shift nanodroplets compared to microbubbles. *J Ther Ultrasound BioMed Central Ltd.*, 2015;3:1–9. [PubMed: 25635224]
- Mullin L, Gessner R, Kwan J, Kaya M, Borden MA, Dayton PA. Effect of anesthesia carrier gas on in vivo circulation times of ultrasound microbubble contrast agents in rats. *Contrast Media Mol Imaging* 2011;6:126–131. [PubMed: 21246710]
- O'Reilly MA, Hyynen K. Ultrasound enhanced drug delivery to the brain and central nervous system. *Int. J. Hyperth NIH Public Access*, 2012. pp. 386–396.
- Pazos V, Mongrain R, Tardif JC. Polyvinyl alcohol cryogel: Optimizing the parameters of cryogenic treatment using hyperelastic models. *J Mech Behav Biomed Elsevier*, 2009;2:542–549. [PubMed: 19627861]
- Rapoport NY, Kennedy AM, Shea JE, Scaife CL, Nam KH. Controlled and targeted tumor chemotherapy by ultrasound-activated nanoemulsions/microbubbles. *J Control Release NIH Public Access*, 2009;138:268–276. [PubMed: 19477208]
- Raut S, Khairalseed M, Honari A, Sirsi SR, Hoyt K. Impact of hydrostatic pressure on phase-change contrast agent activation by pulsed ultrasound. *J Acoust Soc Am* 2019;145:3457–3466. [PubMed: 31255129]
- Rojas JD, Borden MA, Dayton PA. Effect of Hydrostatic Pressure, Boundary Constraints and Viscosity on the Vaporization Threshold of Low-Boiling-Point Phase-Change Contrast Agents. *Ultrasound Med Biol Elsevier*, 2019;45:968–979. [PubMed: 30658858]
- Sheeran PS, Luois S, Dayton PA, Matsunaga TO. Formulation and acoustic studies of a new phase-shift agent for diagnostic and therapeutic ultrasound. *Langmuir American Chemical Society*, 2011a;27:10412–10420. [PubMed: 21744860]
- Sheeran PS, Luois SH, Mullin LB, Matsunaga TO, Dayton PA. Design of ultrasonically-activatable nanoparticles using low boiling point perfluorocarbons. *Biomaterials Biomaterials*, 2012;33:3262–3269. [PubMed: 22289265]
- Sheeran PS, Matsunaga TO, Dayton PA. Phase change events of volatile liquid perfluorocarbon contrast agents produce unique acoustic signatures. *Phys Med Biol Institute of Physics Publishing*, 2014;59:379–401. [PubMed: 24351961]
- Sheeran PS, Rojas JD, Puett C, Hjelmquist J, Arena CB, Dayton PA. Contrast-Enhanced Ultrasound Imaging and in Vivo Circulatory Kinetics with Low-Boiling-Point Nanoscale Phase-Change Perfluorocarbon Agents. *Ultrasound Med Biol Elsevier*, 2015;41:814–831. [PubMed: 25619781]

- Sheeran PS, Wong VP, Luois S, McFarland RJ, Ross WD, Feingold S, Matsunaga TO, Dayton PA. Decafluorobutane as a Phase-Change Contrast Agent for Low-Energy Extravascular Ultrasonic Imaging. *Ultrasound Med Biol NIH Public Access*, 2011b;37:1518–1530. [PubMed: 21775049]
- Shpak O, Verweij M, Vos HJ, De Jong N, Lohse D, Versluis M. Acoustic droplet vaporization is initiated by superharmonic focusing. *Proc Natl Acad Sci U S A National Academy of Sciences*, 2014;111:1697–1702. [PubMed: 24449879]
- Surry KJM, Austin HJB, Fenster A, Peters TM. Poly(vinyl alcohol) cryogel phantoms for use in ultrasound and MR imaging. *Phys Med Biol* 2004;49:5529–5546. [PubMed: 15724540]
- Takegami K, Kaneko Y, Watanabe T, Maruyama T, Matsumoto Y, Nagawa H. Polyacrylamide gel containing egg white as new model for irradiation experiments using focused ultrasound. *Ultrasound Med Biol Ultrasound Med Biol*, 2004;30:1419–1422. [PubMed: 15582242]
- Wan W, Dawn Bannerman A, Yang L, Mak H. Poly(Vinyl Alcohol) Cryogels for Biomedical Applications. *Adv Polym Sci Springer New York LLC*, 2014;263:283–321.
- Weir AJ, Sayer R, Wang CX, Parks S. A wall-less poly(vinyl alcohol) cryogel flow phantom with accurate scattering properties for transcranial Doppler ultrasound propagation channels analysis. *Proc Annu Int Conf IEEE Eng Med Biol Soc EMBS Institute of Electrical and Electronics Engineers Inc.*, 2015. pp. 2709–2712.
- Williams R, Wright C, Cherin E, Reznik N, Lee M, Gorelikov I, Foster FS, Matsuura N, Burns PN. Characterization of Submicron Phase-change Perfluorocarbon Droplets for Extravascular Ultrasound Imaging of Cancer. *Ultrasound Med Biol* 2013;39:475–489. [PubMed: 23312960]

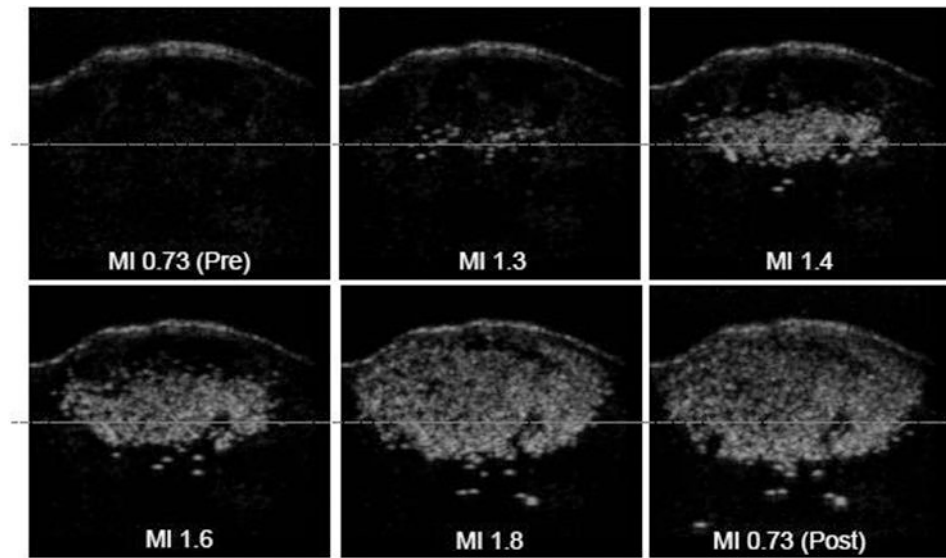


Figure 1. Octafluoropropane (OFP) droplet activation observed in polyvinyl alcohol cryogel (PVA-C) phantoms with increasing mechanical index (MI) at room temperature.

Below the activation pressure threshold, the phantom appears dark (MI 0.73 Pre). Increased signal is observed at the focus (dashed line) as imaging pressure is increased, and the signal remains visible when the imaging pressure is reduced to below the activation threshold (MI 0.73 Post).

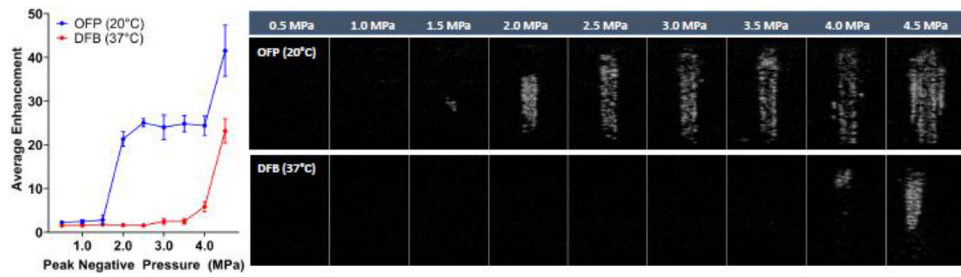


Figure 2. High-intensity focused ultrasound (HIFU)-activated DFB droplets embedded in PVA cryogel.

Octafluoropropane (OFP) and Decafluorbutane (DFB) droplets suspended in polyvinyl alcohol (PVA) cryogels treated with focused ultrasound across a range of ultrasound pressures from 0.5 to 4.5 MPa peak negative pressure (PNP) demonstrated increasing activation with increasing ultrasound pressure. (a) Average enhancement following exposure to various ultrasound parameters ($n=3$). (b) Representative images of OFP (top row) and DFB (bottom row) droplet phantoms following activation.